Hindawi
Mathematical Problems in Engineering
Volume 2018, Article ID 7105872, 11 pages
https://doi.org/10.1155/2018/7105872

Research Article

Model-Free Adaptive Control of Direct Drive Servo Valve of Electromagnetic Linear Actuator

Jianhui Zhu,[1,2] **Jianguo Dai**,[1] **and Cheng Wang**[1]

[1]*Faculty of Transportation Engineering, Huaiyin Institute of Technology, Huai'an 223003, China*
[2]*School of Mechanical Engineering, Nanjing University of Science and Technology, Nanjing 210094, China*

Correspondence should be addressed to Jianhui Zhu; ffxyz505@gmail.com

Received 23 March 2018; Revised 1 September 2018; Accepted 13 September 2018; Published 22 October 2018

Academic Editor: Yuqiang Wu

An electromagnetic linear actuator (EMLA) has a promising application in direct motion control. However, ELMA will inevitably inherit uncertainties in the face of load changes, system parameter perturbation, and inherent system nonlinearities, all of which constitute disturbances adversely affecting the precision and adaptability of the control system. A model-free adaptive control (MFAC) strategy based on full form dynamic linearization (FFDL) was proposed to reduce the sensitivity of the control system to the disturbances. An adaptive control of direct drive servo valve was achieved based on the online interaction of characteristic parameters and control algorithms. The feasibility and precision of the proposed algorithm were verified through simulation and experimental results. The results show that the proposed algorithm could achieve adaptive adjustment of the servo valve response at different openings of 0-3 mm without changing control parameters, with the response time controlled within 10ms and steady state error less than 0.04mm. Furthermore, the proposed algorithm had better robustness and capacity of resisting disturbance.

1. Introduction

Electromagnetic linear actuator (EMLA) has a wide range of applications in the field of linear motion control, because of high-precision, high-response, and nonintermediate conversion [1, 2]. EMLA has been widely applied in electromagnetic engine valve, automatic transmission, and freedom motion platform of six degrees. It has also drawn more and more attention as a part of electrical-mechanical conversion device of direct drive servo valve [3–5].

Currently, many algorithms on the moving control of electromagnetic actuators have been discussed [6]. Typical control algorithms include iterative learning control [7], inverse system method control [8], and sliding mode control [9]. However, for direct drive servo valve, the control algorithm is normally based on accurate modeling for control object, which is very difficult to be achieved; thus control effect is poor [10, 11].

On the other hand, in order to meet the highly responsive requirements, data-driven algorithms, such as the classic PID control, have large differential coefficient and are more likely to cause system instability [12]. For discrete-time nonlinear systems, MFAC (Model-Free Adaptive Control) uses a new dynamic linearization method and a concept of pseudo-partial derivative. MFAC depends only on real-time measurement data of the control system, rather than depending on any mathematical model information of the control system. Through online interactions of characteristic parameters and control algorithms, the amendment of Pan model as well as the ideal control function of system can be achieved [13]. Since proposed by Hou Zhongsheng 20 years ago, MFAC has been used in permanent magnet linear motor [14, 15], freeway traffic systems, wind power plant, some complex industrial processes, etc. [16].

In this paper, a model-free adaptive control strategy was proposed based on full format dynamic linearization to achieve better control effect and high-response. Simulation and test were carried out to verify the adaptive control of ELMA for direct drive servo valve.

2. System Description

The schematic diagram and three-dimensional model of ELMA in direct drive servo valve are shown in Figure 1.

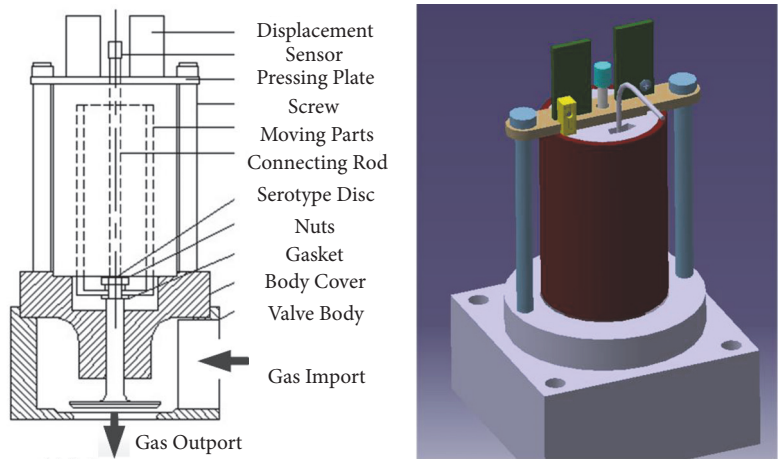

(a) Schematic diagram (b) Three-dimensional model diagram

Figure 1: The schematic diagram and three-dimensional model of EMLA in direct drive servo valve.

It mainly consists of magneto-resistive displacement sensor, electromagnetic linear actuator, poppet valve, seat, and valve cover fixed to the central axis. The gas inlet is connected to the external air fuel supply line.

The electromagnetic linear actuator controls the actuator current and position to achieve double-loop control spool motion through a certain control algorithm, thus controlling the opening of the servo valve connected to spool. Therefore, the spool movement is able to follow the predetermined motion rule.

3. Model-Free Adaptive Controller Design

3.1. Control Algorithm Design. Model-Free adaptive controller is based on "nonparametric model", also known as "pan model". It is worth noting that the term of "model-free" basically refers to the fact that the controller does not need to recognize the global dynamic model of controlled objects. With the help of dynamic linear technology, this model-free adaptive controller builds equivalent dynamic linear data near the work point at each sampling instant. Even though the data model is fictitious, the controller only needs to control the input and output (I/O) data of the object, which is a design method integrating identification and control as a whole [17].

The control system of electromagnetic linear direct drive servo valve can be seen as a single-input and single-output system in discrete time. Input refers to controlled current or voltage signal, while output refers to lift range, that is, valve opening. The general discrete-time single-input single-output (SISO) nonlinear system is expressed as follows [18]:

$$y(k+1) = f\left(y(k), \ldots, y\left(k-n_y\right), u(k), \ldots, u\left(k-n_u\right)\right) \tag{1}$$

where $u(k)$ and $y(k)$ are system input and output at the instant k, n_y and n_u are two unknown positive integers, and f is an unknown nonlinear system.

By utilizing the dynamic linearization method of MFAC theory [19, 20], the nonlinear discrete system can be equivalently converted to a dynamic linear data model based on input and output data increment. Data model based on FFDL (Full Form Dynamic Linearization) can be expressed as

$$\Delta y(k+1) = \Phi^T_{f,L_y,L_u}(k)\,\Delta H_{L_y,L_u}(k) \tag{2}$$

$$\Phi^T_{f,L_y,L_u}(k) = \left[\Phi_1(k), \ldots, \Phi_{L_y}(k), \Phi_{L_y+1}(k), \ldots, \Phi_{L_y+L_u}(k)\right]^T \tag{3}$$

$$\Delta H_{L_y,L_u}(k) = \left[\Delta y(k), \ldots, \Delta y\left(k-L_y+1\right), \Delta u(k), \ldots, \Delta u\left(k-L_u+1\right)\right]^T \tag{4}$$

where $\Delta y(k+1)$ is incremental output at two adjacent moments, $\Phi^T_{f,L_y,L_u}(k)$ is bounded pseudo-gradient, L_y and L_u are system pseudo-orders, $\Phi^T_{f,L_y,L_u}(k)$ is a time-varying parameter vector of pseudo-gradient, and $\Delta H_{L_y,L_u}(k)$ is change vector consisting of all input and output signals in the sliding time window.

Based on this model, the control plan of FFDL-MFAC is

$$\begin{aligned} u(k) &= u(k-1) + \frac{\rho_{L_y+1}\Phi_{L_y+1}(k)\left(y*(k+1) - y(k)\right)}{\lambda + \left|\Phi_{L_y+1}(k)\right|^2} \\ &\quad - \frac{\Phi_{L_y+1}(k)\sum_{i=1}^{L_y}\rho_i\Phi_i(k)\,\Delta y(k-i+1)}{\lambda + \left|\Phi_{L_y+1}(k)\right|^2} \\ &\quad - \frac{\Phi_{L_y+1}(k)\sum_{i=L_y+2}^{L_y+L_u}\rho_i\Phi_i(k)\,\Delta u\left(k-L_y-i+1\right)}{\lambda + \left|\Phi_{L_y+1}(k)\right|^2} \end{aligned} \tag{5}$$

where λ is the weighting factor as well as the penalty factor for controlling input change. The smaller the λ, the faster the system responses, overshoot, or instability that may be generated; on the contrary, the greater the λ is, the more stable the input and output are, and the smaller the overshoot is. ρ_i is step factor, $\rho_i \in (0,1]$, $i = 1, 2, \cdots, L_y + L_u$, which is set to make the control algorithm design more flexible. $y * (k+1)$ is the desired system output.

3.2. PG Vector. The traditional parameter estimation criterion function is to minimize the square of the difference between the system model output and the real output. However, when applying the parameter estimation algorithm derived from such a criterion function, the estimated value of the parameter often changes too fast, or some inaccurate sampled data of mutations (which may be caused by interference or sensor failure) are too sensitive. To this end, for the EMLA system in this paper, the following estimation criterion function is used.

$$\begin{aligned} &\left|J\left(\phi_{f,L_y,L_u}(k)\right)\right| \\ &\quad = \left|\left(y(k) - y(k-1) - \phi^T{}_{f,L_y,L_u}(k)\right)\right|^2 \\ &\quad + \mu\left\|\phi_{f,L_y,L_u}(k) - \hat{\phi}_{f,L_y,L_u}(k)\right\|^2 \end{aligned} \tag{6}$$

According to the optimal condition $\partial J(\phi_{f,Ly,Lu}(k))/\phi_{f,Ly,Lu}(k) = 0$, the upper formula is used to find the extremum of $\phi_{f,Ly,Lu}(k)$, and the matrix inversion lemma is used to obtain the estimation algorithm of PG.

$$\widehat{\Phi}_{f,L_y,L_u}(k) = \widehat{\Phi}_{f,L_y,L_u}(k-1) + \frac{\eta\Delta H_{L_y,L_u}(k-1)\left(y(k) - y(k-1)\right) - \widehat{\Phi}^T_{f,L_y,L_u}(k)\,\Delta H_{L_y,L_u}(k-1)}{\mu + \left\|\Delta H_{L_y,L_u}(k-1)\right\|^2} \tag{7}$$

where μ is a weighting factor, η is a step factor, $\eta \in (0,2]$, and $\widehat{\Phi}_{f,L_y,L_u}(k-1)$ is the estimated value of $\widehat{\Phi}_{f,L_y,L_u}(k)$. If $\|\widehat{\Phi}_{f,L_y,L_u}(k)\| \le \varepsilon$ or $\Delta H_{L_y,L_u}(k-1) \le \varepsilon$, or $\text{sign}(\widehat{\Phi}_{L_y+1}(k)) \ne \text{sign}(\widehat{\Phi}_{L_y+1}(1))$, $\widehat{\Phi}_{f,L_y,L_u}(k) = \widehat{\Phi}_{f,L_y,L_u}(1)$, $\widehat{\Phi}_{f,L_y,L_u}(1)$ is the initial value of $\widehat{\Phi}_{f,L_y,L_u}(k)$. ε is sufficiently small positive integer, which is set to 0.0001 in simulation. Therefore, model-free adaptive control algorithm was established based on full format. With this established algorithm, the controller is designed using the online input and output data measured by closed-loop control system, which does not significantly or implicitly contain any information related to the control system dynamic model.

3.3. Control Scheme. By combining the control algorithm of the previous nonlinear chaotic system and the corresponding pseudo-partial derivative estimation algorithm, the model-free adaptive control scheme of chaotic system can be given as follows.

$$\widehat{\Phi}_{f,L_y,L_u}(k) = \widehat{\Phi}_{f,L_y,L_u}(k-1) + \frac{\eta\Delta H_{L_y,L_u}(k-1)\left(y(k) - y(k-1)\right) - \widehat{\Phi}^T_{f,L_y,L_u}(k)\,\Delta H_{L_y,L_u}(k-1)}{\mu + \left\|\Delta H_{L_y,L_u}(k-1)\right\|^2} \tag{8}$$

$$\begin{aligned} &\left\|\widehat{\Phi}_{f,L_y,L_u}(k)\right\| \le \varepsilon \\ &\text{or } \Delta H_{L_y,L_u}(k-1) \le \varepsilon, \\ &\text{or } \text{sign}\left(\widehat{\Phi}_{L_y+1}(k)\right) \ne \text{sign}\left(\widehat{\Phi}_{L_y+1}(1)\right), \\ &\widehat{\Phi}_{f,L_y,L_u}(k) = \widehat{\Phi}_{f,L_y,L_u}(1) \end{aligned} \tag{9}$$

$$\begin{aligned} u(k) = u(k-1) &+ \frac{\rho_{L_y+1}\Phi_{L_y+1}(k)\left(y*(k+1) - y(k)\right)}{\lambda + \left|\Phi_{L_y+1}(k)\right|^2} - \frac{\Phi_{L_y+1}(k)\sum_{i=1}^{L_y}\rho_i\Phi_i(k)\,\Delta y(k-i+1)}{\lambda + \left|\Phi_{L_y+1}(k)\right|^2} \\ &- \frac{\Phi_{L_y+1}(k)\sum_{i=L_y+2}^{L_y+L_u}\rho_i\Phi_i(k)\,\Delta u\left(k - L_y - i + 1\right)}{\lambda + \left|\Phi_{L_y+1}(k)\right|^2} \end{aligned} \tag{10}$$

In this scheme, the introduction of (9) is to make the pseudo-partial derivative estimation algorithm have stronger ability to track time-varying parameters. In this scheme, only one one-dimensional parameter, i.e., system pseudo-bias, needs to be adjusted online. It can be seen from the control scheme (8)-(10) that the proposed model-free adaptive control scheme only uses the I/O data of the controlled system for controller design, which is basically a data-driven control method. The proposed control scheme is independent of the explicit or implicit dynamic model and system structure information of the controlled system, so it is a control method typically for the modeless nonlinear system.

3.4. Stability Analysis of Algorithm. Before analyzing the robust stability of the above algorithm, the following assumptions are proposed.

Assumption 1. The partial derivative of the function $f(...)$ with respect to the $(n_y + 2)$ variables is continuous except for a finite time point.

Assumption 2. Except for the finite time point, the system satisfies the generalized Lipschitz condition; that is, at any time $k_1 \neq k_2$, $k_1, k_2 \geq 0$, and $u(k_1) \neq u(k_2)$, there is the following relationship:

$$\left|y\left(k_1+1\right)-y\left(k_2+1\right)\right| \leq b\left|u\left(k_1\right)-u\left(k_2\right)\right| \tag{11}$$

$y(k_i + 1) = f(y(k_i), ..., y(k_i - n_y), u(k_i), ..., u(k_i - n_u))$, $i = 1, 2; b > 0$ is a constant.

Assumption 1 is a typical constraint on general nonlinear systems in control system design.

Assumption 2 is a limitation on the upper bound of the system's output rate of change. A bounded input energy change should produce a bounded output energy change within the system.

Assumption 3. For a given bounded desired output signal $y*(k+1)$, there is always a bounded amount $u*(k)$. The system is driven by the control input signal and its output is equal to $*(k+1)$.

Assumption 4. At any time k and $\Delta u(k) \neq 0$, the symbol of the system's PPD remains unchanged; i.e., $\phi_c(k) > \underline{\varepsilon} > 0$, *or* $\phi_c(k) < \underline{-\varepsilon}$, ε is a small positive number.

Assumption 3 is a necessary condition for the design of the control problem; that is, the output of the system is controllable.

Assumption 4 means that the corresponding output of controlled system should be undiminished when the control input is increased, which can be considered as a "quasi-linear" feature of the system.

Theorem 5. *If system (1) satisfies assumptions 1–4, there is a positive number* $\lambda_{\min} > 0$*, so that when* $\lambda > \lambda_{\min}$,

(1) $\lim_{k\longrightarrow\infty}|y* - y(k+1)| = 0$,

(2) $\{y(k)\}$ *and* $\{u(k)\}$ *are bounded sequence.*

Proof. Define $\tilde{\phi}_{f,Ly,Lu}(k) = \hat{\phi}_{f,Ly,Lu}(k) - \phi_{f,Ly,Lu}(k)$ as the pseudo-partial derivative estimation error of the control algorithm. In the parameter estimation algorithm (8), by subtracting the terminal with $\hat{\phi}_{f,Ly,Lu}(k)$, we can obtain the following.

$$\begin{aligned}\tilde{\phi}_{f,Ly,Lu}(k) &= \hat{\phi}_{f,Ly,Lu}(k-1) + \frac{\eta\Delta u(k-1)}{\mu+\Delta u(k-1)^2} \\ &\quad\times\left(\Delta y(k) - \hat{\phi}_{f,Ly,Lu}(k-1)\Delta u(k-1)\right) \\ &\quad - \phi_{f,Ly,Lu}(k)\end{aligned} \tag{12}$$

By substituting $\Delta y(k) = \phi_{f,Ly,Lu}(k-1)\Delta u(k-1)$ into expressions:

$$\begin{aligned}\tilde{\phi}_{f,Ly,Lu}(k) &= \hat{\phi}_{f,Ly,Lu}(k-1) - \phi_{f,Ly,Lu}(k-1) \\ &\quad + \frac{\eta\Delta u(k-1)}{\mu+\Delta u(k-1)^2}\times\left(\phi_{f,Ly,Lu}(k-1)\Delta u(k-1)\right. \\ &\quad \left. - \hat{\phi}_{f,Ly,Lu}(k-1)\Delta u(k-1)\right) + \phi_{f,Ly,Lu}(k-1) \\ &\quad - \phi_{f,Ly,Lu}(k)\end{aligned} \tag{13}$$

due to the expression $\tilde{\phi}_{f,Ly,Lu}(k-1) = \hat{\phi}_{f,Ly,Lu}(k-1) - \phi_{f,Ly,Lu}(k-1)$, we can obtain the following.

$$\begin{aligned}\tilde{\phi}_{f,Ly,Lu}(k) &= \left(1 - \frac{\eta\Delta u(k-1)^2}{\mu+\Delta u(k-1)^2}\right)\tilde{\phi}_{f,Ly,Lu}(k-1) \\ &\quad + \phi_{f,Ly,Lu}(k-1) - \phi_{f,Ly,Lu}(k)\end{aligned} \tag{14}$$

By taking absolute values on both sides of (14), there is the following.

$$\begin{aligned}\left|\tilde{\phi}_{f,Ly,Lu}(k)\right| &\leq \left|1 - \frac{\eta\Delta u(k-1)^2}{\mu+\Delta u(k-1)^2}\right|\left|\tilde{\phi}_{f,Ly,Lu}(k-1)\right| \\ &\quad + \left|\phi_{f,Ly,Lu}(k-1) - \phi_{f,Ly,Lu}(k)\right|\end{aligned} \tag{15}$$

Since $\Delta u(k) \neq 0$, when $0 < \eta \leq 1$ 0 and $\mu \geq 0$, there is a constant d_1, which satisfies the following.

$$0 \leq \left|\left(1 - \frac{\eta\Delta u(k-1)^2}{\mu+\Delta u(k-1)^2}\right)\right| \leq d_1 < 1 \tag{16}$$

On the other hand, based on Assumption 2, we get $|\phi_{f,Ly,Lu}(k)| \leq b$, so $|\phi_{f,Ly,Lu}(k-1) - \phi_{f,Ly,Lu}(k)| \leq 2b$. According to (15) and (16), the following recursive inequalities can be obtained.

$$\begin{aligned}\left|\tilde{\phi}_{f,Ly,Lu}(k)\right| &\leq d_1\left|\tilde{\phi}_{f,Ly,Lu}(k-1)\right| + 2b \\ &\leq d_1^2\left|\tilde{\phi}_{f,Ly,Lu}(k-2)\right| + 2d_1 b + 2b \leq \ldots \\ &\leq d_1^{k-1}\left|\tilde{\phi}_{f,Ly,Lu}(1)\right| + \frac{2b\left(1-d_1^{k-1}\right)}{1-d_1}\end{aligned} \tag{17}$$

The above formula indicates that $\widetilde{\phi}_{f,Ly,Lu}(k)$ is bounded. Since $|\phi_{f,Ly,Lu}(k)| \le b$ is bounded, $\widehat{\phi}_{f,Ly,Lu}(k)$ is bounded.

Define the tracking error of the system as

$$e(k+1) = y^* - y(k+1) \tag{18}$$

$$\begin{aligned} |e(k+1)| &= \left|y^* - y(k+1)\right| \\ &= \left|y^* - y(k) - \phi_{f,Ly,Lu}(k)\,\Delta u(k)\right| \\ &\le \left|1 - \frac{\rho\phi_{f,Ly,Lu}(k)\,\widehat{\phi}_{f,Ly,Lu}(k)}{\lambda + \left|\widehat{\phi}_{f,Ly,Lu}(k)\right|^2}\right| |e(k)| \end{aligned} \tag{19}$$

From assumption 4 and (9), $\phi_{f,Ly,Lu}(k)\widehat{\phi}_{f,Ly,Lu}(k) \ge 0$.

Let $\lambda_{\min} = b^2/4$. Using the inequality $\alpha^2 + \beta^2 \ge 2\alpha\beta$ and choosing $\lambda > \lambda_{\min}$, there is a constant $M_1 (0 < M_1 < 1)$ such that the following holds:

$$\begin{aligned} 0 < M_1 &\le \frac{\phi_{f,Ly,Lu}(k)\,\widehat{\phi}_{f,Ly,Lu}(k)}{\lambda + \left|\widehat{\phi}_{f,Ly,Lu}(k)\right|^2} \le \frac{b\widehat{\phi}_{f,Ly,Lu}(k)}{\lambda + \left|\widehat{\phi}_{f,Ly,Lu}(k)\right|^2} \\ &\le \frac{b\widehat{\phi}_{f,Ly,Lu}(k)}{2\sqrt{\lambda}\widehat{\phi}_{f,Ly,Lu}(k)} < \frac{b}{2\sqrt{\lambda_{\min}}} = 1 \end{aligned} \tag{20}$$

where b is the constant that satisfies the conclusion of theorem $|\phi_{f,Ly,Lu}(k)| \le b$.

According to (20), $0 < \rho < 1$ and $\lambda < \lambda_{\min}$, there must be a constant $\mathrm{d}_2 (d_2 < 1)$, so that

$$\begin{aligned} &\left|1 - \frac{\rho\phi_{f,Ly,Lu}(k)\,\widehat{\phi}_{f,Ly,Lu}(k)}{\lambda + \left|\widehat{\phi}_{f,Ly,Lu}(k)\right|^2}\right| \\ &\quad = 1 - \frac{\rho\phi_{f,Ly,Lu}(k)\,\widehat{\phi}_{f,Ly,Lu}(k)}{\lambda + \left|\widehat{\phi}_{f,Ly,Lu}(k)\right|^2} \le 1 - \rho M_1 \triangleq \mathrm{d}_2 \\ &\quad < 1 \end{aligned} \tag{21}$$

Combining (19) and (21), there is the following.

$$\begin{aligned} |e(k+1)| &\le d_2 |e(k)| \le d_2^2 |e(k-1)| \le \ldots \\ &\le d_2^k |e(1)|. \end{aligned} \tag{22}$$

The above formula means that Theorem 5 (1) holds; that is, the control algorithm can control the ELMA to the desired output. In addition, since $y^*(k)$ is a constant, $e(k)$ converges to mean $y(k)$ bounded. Using $(\sqrt{\lambda})^2 + |\widehat{\phi}_{f,Ly,Lu}(k)|^2 \ge 2\sqrt{\lambda}\widehat{\phi}_{f,Ly,Lu}(k)$ and $\lambda > \lambda_{\min}$, the following inequality is given by (10):

$$\begin{aligned} |\Delta u(k)| &= \left|\frac{\rho\widehat{\phi}_{f,Ly,Lu}(k)\left(y^* - y(k)\right)}{\lambda + \left|\widehat{\phi}_{f,Ly,Lu}(k)\right|^2}\right| \\ &\le \left|\frac{\rho\widehat{\phi}_{f,Ly,Lu}(k)}{\lambda + \left|\widehat{\phi}_{f,Ly,Lu}(k)\right|^2}\right| |e(k)| \\ &\le \left|\frac{\rho\widehat{\phi}_{f,Ly,Lu}(k)}{2\sqrt{\lambda}\widehat{\phi}_{f,Ly,Lu}(k)}\right| |e(k)| \le \left|\frac{\rho}{2\sqrt{\lambda_{\min}}}\right| |e(k)| \\ &= M_2 |e(k)| \end{aligned} \tag{23}$$

where M2 = ρ is a bounded constant. Based on (22) and (23), the following equation can be obtained.

$$\begin{aligned} |u(k)| &\le |u(k) - u(k-1)| + |u(k-1)| \\ &\le |u(k) - u(k-1)| + |u(k-1) - u(k-2)| \\ &\quad + |u(k-2)| \\ &\le |\Delta u(k)| + |\Delta u(k-1)| + \ldots + |\Delta u(2)| + |u(1)| \\ &\le M_2 (|e(k)| + |e(k-1)| + \ldots + |e(2)|) + |u(1)| \\ &\le M_2 \left(d_2^{k-1} |e(1)| + d_2^{k-2} |e(1)| + \ldots + d_2 |e(2)|\right) \\ &\quad + |u(1)| < M_2 \frac{d_2}{1 - d_2} |e(1)| + |u(1)| \end{aligned} \tag{24}$$

Equation (24) indicates that Theorem 5 (2) holds; that is, the system is stable.

In order to obtain input and output (I/O) data required by control algorithm, it is needed to establish a time-varying model. This time-varying model is only used to generate I/O data and to achieve online interaction of data, rather than participating in controller design. Therefore, the system parameters change has no effect on the controller. The nonlinear time-varying model for the motion equation of ELMA direct drive servo valve is described as:

$$\dot{x}(t) = v(t) \tag{25}$$

$$f(t) = K_f i(t) \tag{26}$$

$$u(t) = K_e \dot{x}(t) + Ri(t) + \frac{Ldi(t)}{dt} \tag{27}$$

$$f(t) = m\ddot{x}(t) + f_{load}(t) + f_{friction}(\dot{x}) + \omega(t) \tag{28}$$

$$f_{friction}(\dot{x}) = \left(f_c + \left(f_s - f_c\right) e^{-(\dot{x}/x_s)^\delta} + f_v\dot{x}\right) \mathrm{sign}(\dot{x}) \tag{29}$$

where $f_{friction}$ is friction (N), $f_{load}(t)$ is load force (N), $u(t)$ is control voltage (v), $f(t)$ is actuator force (N), $x(t)$ is actuator position (m), $v(t)$ is the velocity of actuator(m/s), K_f is actuator force constant (N/A), K_e is counter electromotive force constant (V/m/s), R is actuator coil resistance (Ω), sign is sign function, L is coil inductance (H), $i(t)$ is coil current

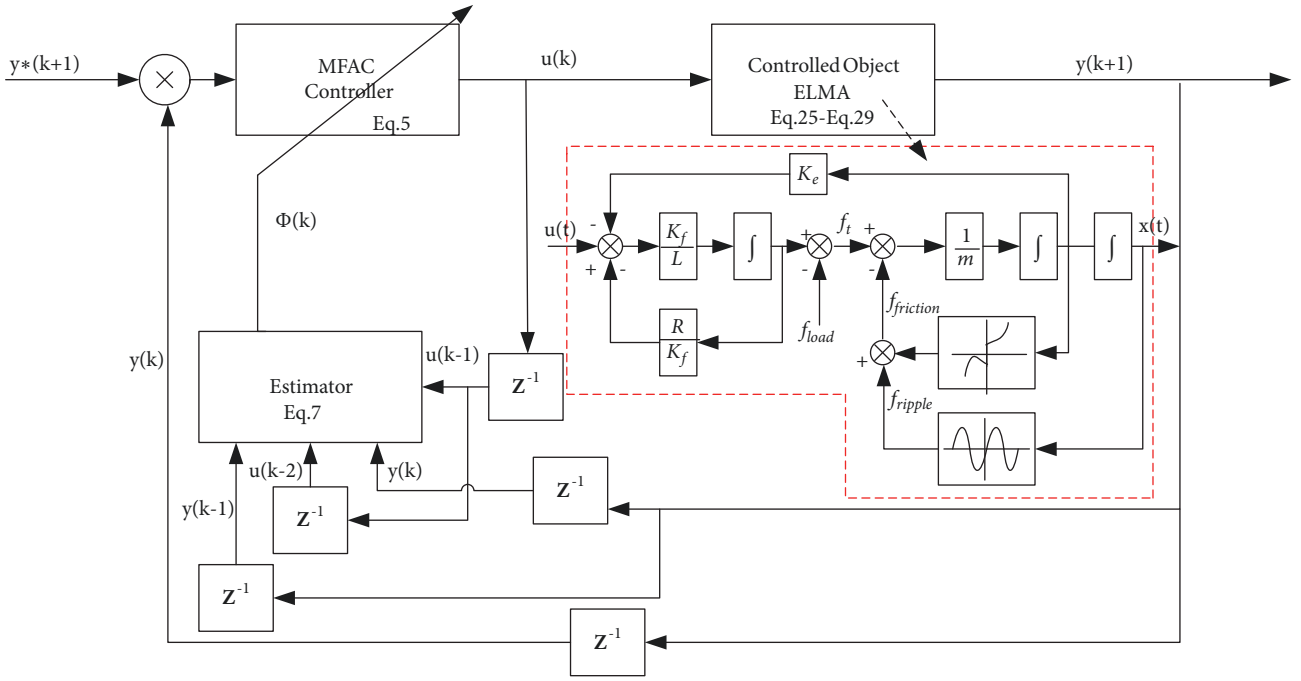

Figure 2: Structure diagram of controller.

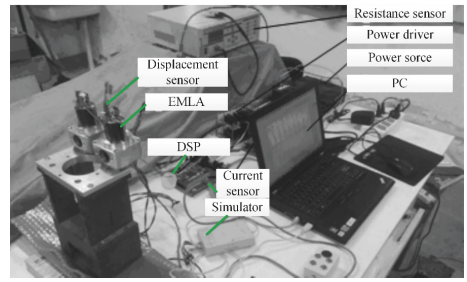

Figure 3: Test platform.

(A), m is moving mass (Kg), $\omega(t)$ is other disturbances, f_s is static friction (N), f_c is coulomb friction (N), x_s is lubrication parameters (m/s), f_v is dynamic friction coefficient (N/m/s), and δ is empirical parameters, which is set to 1 in simulation.

First of all, simulation was carried out to verify the feasibility of the proposed algorithm. The block diagram of controller is shown as Figure 2. It can be seen that the controller mainly consists of model-free adaptive controller module for generating control quantity $u(k)$, estimator module for estimating the algorithm in pseudo-gradient vector, the controlled object- direct drive servo valve of EMLA, and submodule constituted by the nonlinear model. On the basis of model framework, the model of control algorithm was established using software Matlab/Simulink, and simulation of the given fixed lift range and continuous lift range was carried out.

The simulation parameter values are shown in Table 1. Parameters of control algorithm are set as follows: weighting factor $\mu = 1$, step factor $\eta = 2$, $\varepsilon = 0.0001$, and weighting factor $\lambda = 1.2e - 6$. Among them, μ is penalty factor for the control of estimated parameter variation, which is used to limit the linear dynamic range of alternatives; λ is to limit the change of controlled variables, so parameter μ and λ are critical adjustment parameters in controlling, which have a direct impact on the final control results. Step factor is $\rho_6 = [0.1, 0.1, 0.1, 0.1, 0.02, 0.1, 0.1]$, $L_y = 3$ and $L_u = 3$, the initial value of $\widehat{\Phi}_{f,L_y,L_u}(k)$ is $\widehat{\Phi}_{f,L_y,L_u}(1) = [0.03, 0.03, 0.03, 0.03, 0.03, 0.03]^T$, and the sampling period of simulation is 0.0001s. □

4. Results and Analysis

4.1. Experimental System. To further verify the control effect of full format model-free adaptive control algorithm for the EMLA of direct drive servo valve system, the test platform was established, as shown in Figure 3. It consists of DSP2812 controller, power driver circuit, H-bridge, current sensor, magneto-resistive displacement sensor, direct drive servo valve, host computer PC, and power source.

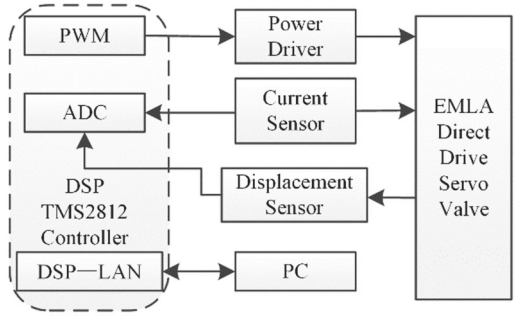

Figure 4: Block diagram of experiment bench and main controller.

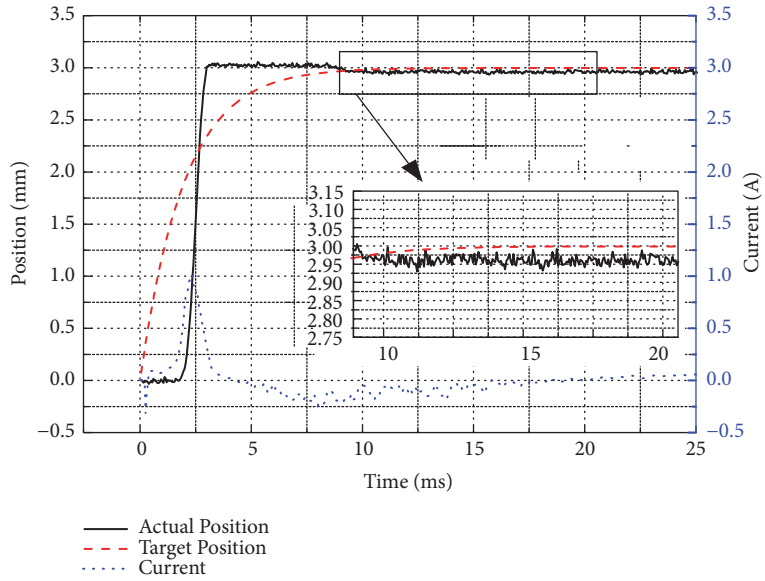

Figure 5: Response and current when target location is 3mm.

Table 1: Prototype parameters.

Parameter Name / Unit	Value
Actuator Coil Resistance/Ω	0.45
Coil Inductance/mH	1.6
Moving Mass/Kg	0.036
Actuator Force Constant/(N/A)	10.8
Counter Electromotive Force Constant/(V/m/s)	10.8
Dynamic Friction Coefficient/(N/m/s)	10

The composition of controller section is shown as Figure 4. The PWM control signals, which are generated by algorithm program of DSP controller, are transmitted to the drive circuit to drive direct drive servo valve of EMLA. At the same time, signals collected by the displacement sensor and the current sensor are fed back to the controller section though A/D converter, forming a closed-loop control. Using the LAN interface of DSP Ethernet, the communication between the upper and slaver computer can be realized, so that functions such as signal input and output, display, and save can be realized.

4.2. Response and Precision Analysis. The experimental verification of control algorithm is conducted based on the built test platform, and test parameters are set as follows: control amount u is current, of which the initial state is set as $u(1) = u(2) = \cdots u(6) = 0$, output y is the valve opening $y(1) = y(2) = \cdots = y(6) = 0$, pseudo-order of full format model-free adaptive control algorithm is set as $L_y = 3$ and $L_u = 3$, step factor and weighting factors are separately set as $\lambda = 0.5$, $\mu = 1$, $\eta = 1$, $\varepsilon = 0.001$, $\rho[1] = [4; 4; 0.9; 0.098; 0.05; 0.05]$, and the initial value of the pseudo-gradient vector is $\phi[1] = [1; 1; 1; 1; -1; -1]$.

During the test, the control parameters are adjusted within a fixed lift range of 3mm, until the output reaches satisfactory results. Then, without changing the parameters, lift range is adjusted in order to verify the algorithm's adaptability to other target lift range. When the target position is 3mm, the response and current are shown as Figure 5; the target location, the output position of actual control, and error are shown as Figure 6.

As can be seen from Figures 5 and 6, within the lift range of 3mm, response time is 4-5ms, steady state phase can be reached after 10ms, the maximum error is 0.0655mm,

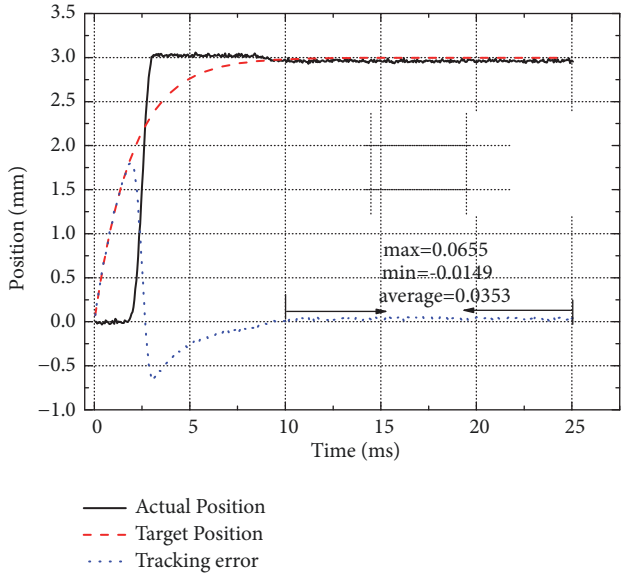

Figure 6: Target position, actual position, and tracking error.

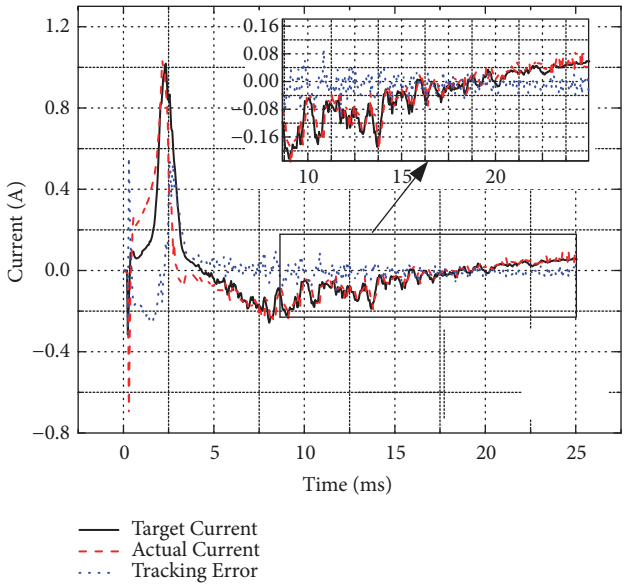

Figure 7: Target current, actual current, and tracking error.

the minimum error is -0.0149mm, and the average error is 0.0353mm. Error tends to exhibit constant decrease. When target location is 3mm, the change of control current and tracking error are shown as Figure 7.

As can be seen from Figure 7, the calculated control current is in good agreement with the actual current collected by sensor, the control peak is less than 1A, and current tracking error continues to decrease to almost zero.

In order to verify the adaptability of algorithm to any other lift ranges, output results were investigated under the condition of different lift ranges. In order to facilitate the drawing, only the output results within lift range of 0.5-3mm were given, i.e., 6 major output results by lift range

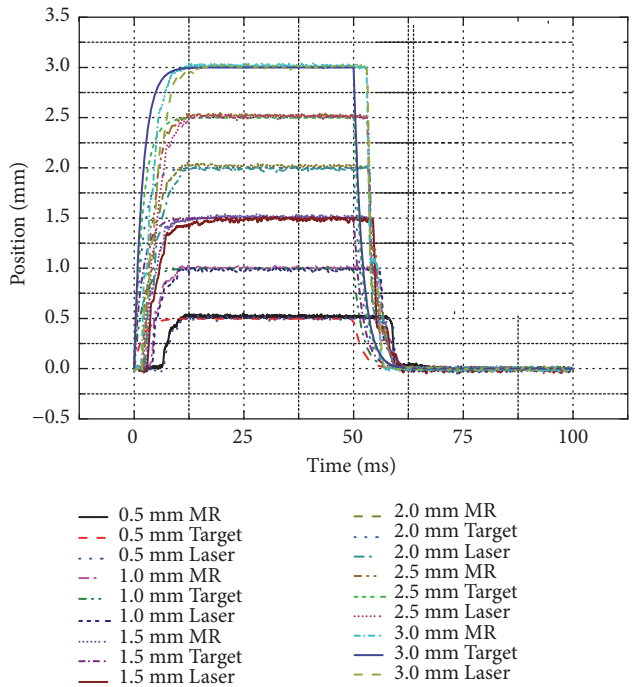

Figure 8: Response output within lift range of 0-3mm.

interval of 0.5mm (0.5, 1.0, 1.5, 2.0, 2.5, 3.0). In addition, tests were carried out by life range interval of 0.1mm. At the same time, in order to verify the control accuracy, the results were compared with laser displacement sensors. As shown in Figure 8, the valve enters into steady state phase after 10ms in all cases, with average error less than 0.04mm.

4.3. Adaptability Analysis of Disturbances. To further verify the robustness of the proposed algorithm, simulation system response under load and no-load, simulation verification was carried out within a lift range of 2mm. The simulation model was verified in our previous work [4]. The system response under load force of 5N and 10N is shown in Figure 9.

Figure 9(a) shows output response within lift range of 2mm. As can be seen from the figure a, with the increase of load, system moves a short distance in the opposite direction to the initial position, and system response becomes slow gradually. Figure 9(b) shows the change of control amount. With the increase of load, the required control amount was also increased to reach the designated target displacement. Figures 9(c) and 9(d) show corresponding speed and current changes. It can be seen that, with the increase in the load, the speed response became slow gradually, and the required current continued to increase. Upon reaching steady state, current and control amount were no longer zero without load, but maintained at a certain value, in order to overcome the load force in the opposite direction.

From the simulation results, it can be known that the control algorithm has good adaptability with the increase of load on the servo valve. Under the same parameters, the

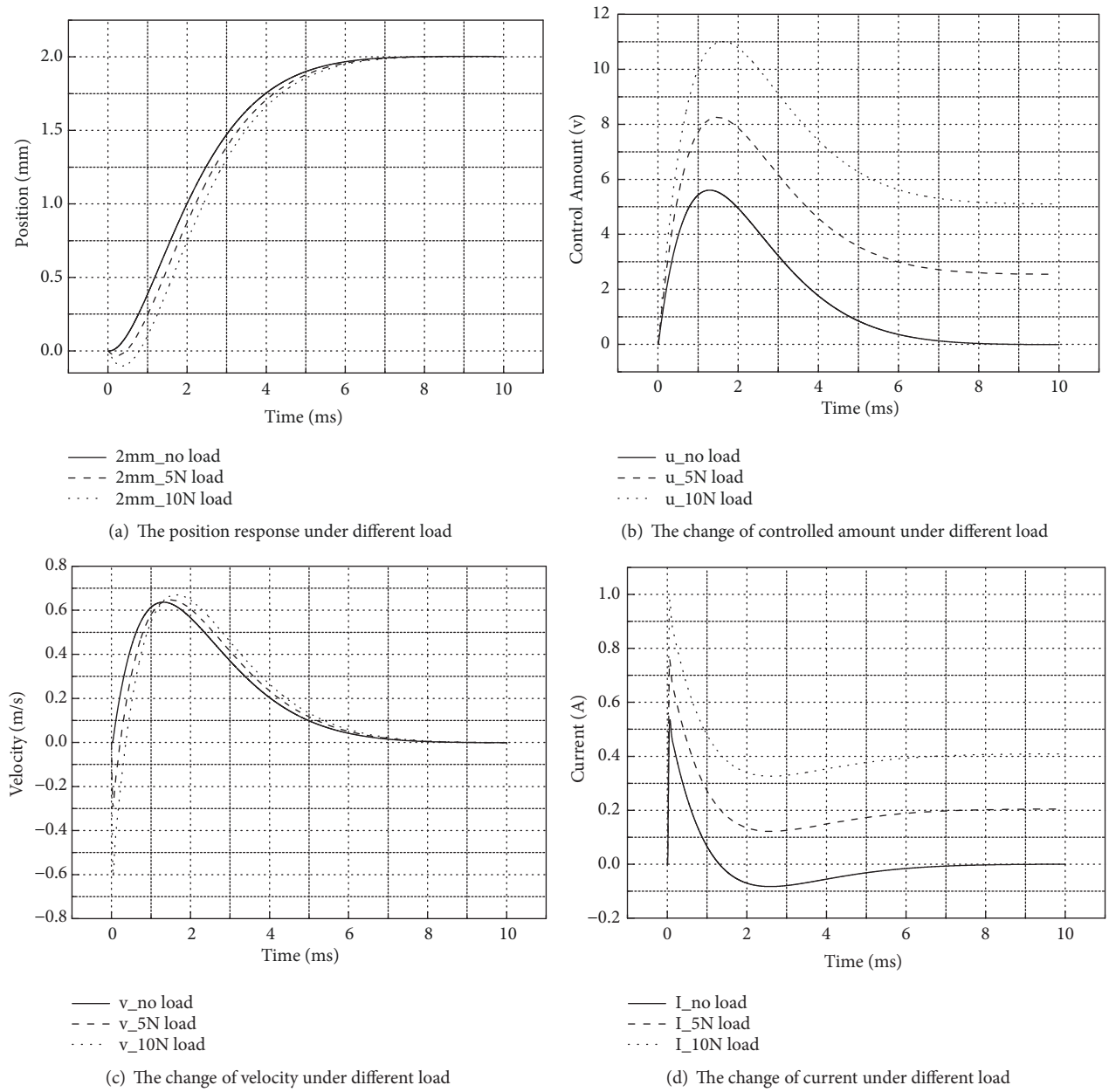

(a) The position response under different load

(b) The change of controlled amount under different load

(c) The change of velocity under different load

(d) The change of current under different load

Figure 9: Response and output of the system with the increase of load force.

proposed control algorithm can accurately reach the target position, with smaller overshoot and higher precision.

In order to verify the suppression on interference, the system response with load disturbance force $\omega(t) = \pm 100N$ within the lift range of 2mm and at motion time of 8-8.5ms was investigated, as shown in Figure 10. As can be seen from the figure, after applying the disturbing force, the system quickly recovered to a stable state, with overshoot less than 4%, indicating a strong anti-interference ability. Similar simulation results were observed within other lift range. The algorithm proposed in this paper for the direct drive servo valve of EMLA has better robustness and capacity of resisting disturbance than the algorithm in [4–6].

5. Conclusion

A model-free adaptive control algorithm based on full format dynamic linearization was built. Through simulation analysis of system step response within different lift ranges as well as investigation of system outputs under increasing load force and disturbances, the application possibility of proposed algorithm in controlling direct drive servo valve of EMLA was verified. By using the full format model-free adaptive control algorithm, tests on actual control of the direct drive servo valve of EMLA were carried out. The simulation and test results show that the proposed algorithm could achieve adaptive adjustment of the servo valve response at different openings of 0-3mm, with the response time controlled within

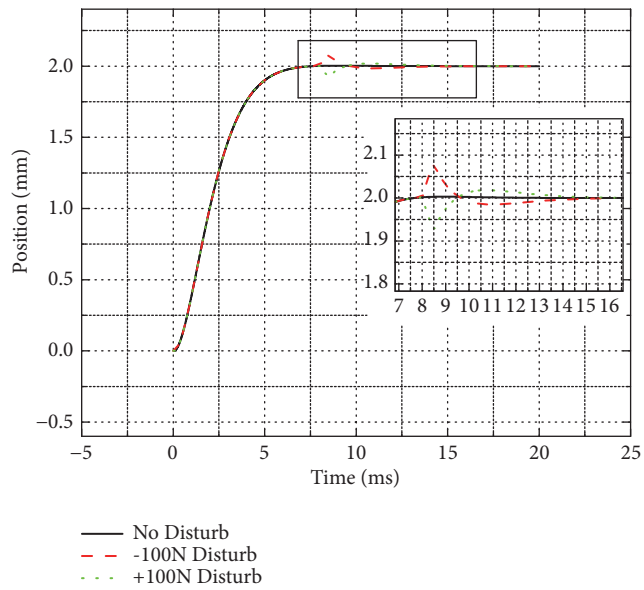

Figure 10: System response with the increase of disturbance.

10ms, and steady state error less than 0.04mm. Furthermore, the proposed algorithm has better robustness and capacity of resisting disturbance and achieves the purpose of servo control without changing controller parameters.

Data Availability

The data used to support the findings of this study are available from the corresponding author upon request.

Conflicts of Interest

The authors declare that they have no conflicts of interest.

Acknowledgments

This work was supported by the National Natural Science Foundation of China (Grant No. 51605183, 51505171), Natural Science Foundation of Colleges in Jiangsu Province (Grant No. 15KJB460003), and Science and Technology Support Programs of Huai'an (Grant No. HAG201603).

References

[1] X. Shi and S. Chang, "Extended state observer-based time-optimal control for fast and precise point-to-point motions driven by a novel electromagnetic linear actuator," *Mechatronics*, vol. 23, no. 4, pp. 445–451, 2013.

[2] K. E. Hideki, A. S. Borges, A. A. Cavalini, and V. S. Tr, "Numerical and experimental modal control of flexible rotor using electromagnetic actuator," *Mathematical Problems in Engineering*, vol. 2014, Article ID 361418, 14 pages, 2014.

[3] L. Liu and S. Chang, "Motion control of an electromagnetic valve actuator based on the inverse system method," *Proceedings of the Institution of Mechanical Engineers, Part D: Journal of Automobile Engineering*, vol. 226, no. D1, pp. 85–93, 2012.

[4] J. H. Zhu and S. Q. Chang, "Adaptive inverse system control of electromagnetic linear actuator," *International Journal of Control and Automation*, vol. 8, no. 12, pp. 131–144, 2015.

[5] S. Wu, R. Burton, Z. Jiao, J. Yu, and R. Kang, "Feasibility study on the use of a voice coil motor direct drive flow rate control valve," in *Proceedings of the 2009 ASME Dynamic Systems and Control Conference, DSCC2009*, pp. 621–628, October 2009.

[6] K. S. Peterson and A. G. Stefanopoulou, "Extremum seeking control for soft landing of an electromechanical value actuator," *Automatica*, vol. 40, no. 6, pp. 1063–1069, 2004.

[7] A. G. Espinosa, J.-R. R. Ruiz, and X. A. Morera, "A sensorless method for controlling the closure of a contactor," *IEEE Transactions on Magnetics*, vol. 43, no. 10, pp. 3896–3903, 2007.

[8] P. Mercorelli, "An antisaturating adaptive preaction and a slide surface to achieve soft landing control for electromagnetic actuators," *IEEE/ASME Transactions on Mechatronics*, vol. 17, no. 1, pp. 76–85, 2012.

[9] Y.-P. Yang, J.-J. Liu, D.-H. Ye, Y.-R. Chen, and P.-H. Lu, "Multiobjective optimal design and soft landing control of an electromagnetic valve actuator for a camless engine," *IEEE/ASME Transactions on Mechatronics*, vol. 18, no. 3, pp. 963–972, 2013.

[10] X. Bu, F. Yu, Z. Hou, and H. Zhang, "Model-free adaptive control algorithm with data dropout compensation," *Mathematical Problems in Engineering*, vol. 2012, Article ID 329186, 14 pages, 2012.

[11] H. Zhou, D. Xu, and B. Jiang, "Model free command filtered backstepping control for marine power systems," *Mathematical Problems in Engineering*, vol. 2015, Article ID 619430, 8 pages, 2015.

[12] X. X. Shi, H. S. Li, and J. C. Huang, "A practical scheme for induction motor modelling and speed control," *International Journal of Control & Automation*, vol. 7, no. 4, pp. 113–124, 2014.

[13] Z. S. Hou, "On model-free adaptive control: the state of the art and perspective," *Control Theory & Application*, vol. 23, no. 4, pp. 586–592, 2006.

[14] R. Cao, H. Zhou, Z. Hou et al., "A robust controller based on advance model-free adaptive method for linear motion

systems," in *Proceedings of the 11th World Congress on Intelligent Control and Automation*, pp. 397–402, 2014.

[15] K. K. Tan, T. H. Lee, H. F. Dou, S. J. Chin, and S. Zhao, "Precision motion control with disturbance observer for pulsewidth-modulated-driven permanent-magnet linear motors," *IEEE Transactions on Magnetics*, vol. 39, no. 3, pp. 1813–1818, 2013.

[16] X. P. Lu, W. Li, and Y. G. Lin, "Load Control of Wind Turbine Based on Model-free Adaptive Controller," *Transactions of the Chinese Society for Agricultural Machinery*, vol. 42, no. 2, pp. 109–114, 2011.

[17] K. K. Tan, T. H. Lee, S. N. Huang, and F. M. Leu, "Adaptive-predictive control of a class of SISO nonlinear systems," *Dynamics and Control*, vol. 11, no. 2, pp. 151–174, 2001.

[18] Z. Hou and Y. Zhu, "Controller-dynamic-linearization-based model free adaptive control for discrete-time nonlinear systems," *IEEE Transactions on Industrial Informatics*, vol. 9, no. 4, pp. 2301–2309, 2013.

[19] Z. S. Hou and J. X. Xu, "On data-driven control theory: the state of the art and perspective," *Acta Automatica Sinica*, vol. 35, no. 6, pp. 650–667, 2009.

[20] Z. Hou and X. Bu, "Model free adaptive control with data dropouts," *Expert Systems with Applications*, vol. 38, no. 8, pp. 10709–10717, 2011.